Radiology: Cardiothoracic Imaging

ORIGINAL RESEARCH

Donor and Recipient Characteristics in Heart Transplantation Are Associated with Altered Myocardial Tissue Structure and Cardiac Function

Ryan S. Dolan, MD • Amir A. Rahsepar, MD • Julie Blaisdell, MS • Roberto Sarnari, MD • Kambiz Ghafourian, MD, MPH • Jane E. Wilcox, MD, MSc • Sadiya S. Khan, MD, MSc • Esther E. Vorovich, MD • Jonathan D. Rich, MD • Clyde W. Yancy, MD • Allen S. Anderson, MD • James C. Carr, MD • Michael Markl, PhD

From the Department of Radiology, Northwestern University Feinberg School of Medicine, 737 N Michigan Ave, Suite 1600, Chicago, IL 60611 (R.S.D., A.A.R., J.B., R.S., J.C.C., M.M.); Department of Cardiology, Northwestern University, Chicago, Ill (K.G., J.E.W., S.S.K., E.E.V., J.D.R., C.W.Y., A.S.A.); and Department of Biomedical Engineering, McCormick School of Engineering, Northwestern University, Evanston, Ill (M.M.). Received January 16, 2019; revision requested March 14; final revision received August 6; accepted September 9. **Address correspondence to** R.S.D. (e-mail: *rsdolan1@gmail.com*).

Supported by the National Institutes of Health (National Heart, Lung, and Blood Institute) (grant R01 HL117888).

Conflicts of interest are listed at the end of this article.

Radiology: Cardiothoracic Imaging 2019; 1(5):e190009 • https://doi.org/10.1148/ryct.2019190009 • Content codes: CA MR

Purpose: To use structure-function cardiac MRI in the evaluation of relationships between donor and heart transplantation (HTx) recipient characteristics and changes in cardiac tissue structure and function. HTx candidates and donor hearts are evaluated for donor-recipient matches to improve survival, but the impact of donor and recipient characteristics on changes in myocardial tissue and function in the transplanted heart is not fully understood.

Materials and Methods: Cardiac MRI at 1.5 T was performed from August 2014 to June 2017 in 58 HTx recipients (mean age, 51.1 years ± 12.6 [standard deviation], 26 female patients) and included T2 mapping (to evaluate edematous and/or inflammatory changes), precontrast and postcontrast T1 mapping (allowing the calculation of extracellular volume fraction [ECV] to estimate interstitial expansion), and tissue phase mapping (allowing the calculation of myocardial velocities and twist). Donor and recipient demographics (age, sex, height, weight, and body mass index [BMI]) and comorbidities (hypertension, diabetes, and smoking history) were evaluated for relationships with cardiac MRI measures.

Results: Sex-influenced cardiac MRI measures of myocardial tissue and function are as follows: Female HTx recipients demonstrated increased precontrast T1 ($P = .002$) and reduced systolic peak long-axis velocities ($P = .015$). Increased age of the donor heart was associated with elevated T2 ($r = 0.32$; $P < .05$) and ECV ($r = 0.47$; $P < .01$), indicating increased edema and interstitial expansion, as well as impaired diastolic peak long-axis velocities ($r = 0.41$; $P < .01$). Recipient-donor differences in age, weight, and BMI were significantly associated with elevated ECV ($r = 0.36$–0.48; $P < .05$). Hypertension in donors resulted in increased ECV (31.0% ± 4.2 vs 26.0% ± 3.3; $P = .001$).

Conclusion: Donor and HTx recipient characteristics were significantly associated with cardiac MRI–derived measures of myocardial tissue structure and function.

Heart transplantation (HTx) is performed in nearly 5000 patients with advanced heart failure annually (1). HTx candidates and donor hearts are carefully evaluated to determine which donor-recipient matches have the highest chances of survival. Considerations include the assessment of the donor heart (eg, age and comorbidities) and matching to the characteristics of the recipient (eg, sex and size matching) (2,3). Previous studies have shown that mismatched donor-recipient characteristics (eg, sex and weight) are associated with increased mortality (4–6) and increased risk of acute cardiac allograft rejection (ACAR) and cardiac allograft vasculopathy (CAV) (7,8). Other individual demographic factors, such as donor age, sex, and body size (7,8), or comorbidities, such as donor hypertension (HTN), diabetes mellitus (DM), and smoking, are associated with increased post-HTx mortality (9,10).

Nonetheless, little is understood regarding the impact of donor and recipient factors on global and regional changes in cardiac tissue structure and function. Cardiac MRI is a useful tool for cardiac allograft surveillance due to its ability to quantify changes in global and regional myocardial tissue structure and function. Cardiac MRI techniques include left ventricular (LV) two-dimensional cine steady-state free precession (SSFP) imaging to assess global cardiac function (11,12), T2 mapping to evaluate the composition of the myocardium related to water or fat content such as edematous and inflammatory myocardial change (13,14), precontrast and postcontrast T1 mapping to calculate extracellular volume fraction (ECV) for the assessment of interstitial changes such as myocardial fibrosis (15–17), and tissue phase mapping (TPM) (18,19) for the quantification of regional myocardial velocities and twist. Although some studies have examined associations between demographic factors and cardiac MRI measures of structure and function in the general population, no dedicated studies have investigated the influence of donor and recipient characteristics on cardiac MRI structural and functional measures of cardiac health. Subtle alterations

Abbreviations

ACAR = acute cardiac allograft rejection, BMI = body mass index, CAV = cardiac allograft vasculopathy, DM = diabetes mellitus, ECV = extracellular volume fraction, GFR = glomerular filtration rate, HTN = hypertension, HTx = heart transplantation, LV = left ventricle, SSFP = steady-state free precession, TPM = tissue phase mapping

Summary

Donor and recipient characteristics (such as age, sex, height, weight, and body mass index) and comorbidities (such as hypertension) are associated with global and regional changes in myocardial tissue structure and function measured by using cardiac MRI.

Key Points

- Donor and recipient characteristics (age, sex, height, weight, and body mass index [BMI]), in particular, donor-recipient mismatches of these characteristics, are associated with cardiac MRI–derived measures of edema and/or inflammation, interstitial expansion and/or fibrosis, and systolic and diastolic dysfunction, suggesting the importance of careful donor selection and donor-recipient matching for improved regional tissue structure and functional performance.
- In contrast to current models focusing on age, sex, and weight for donor-recipient matching, additional consideration of height, BMI, and possible comorbidities such as hypertension may be prudent, given the association between these factors and structural and functional changes.

in regional and global cardiac structure (as demonstrated by increased T2, T1, and ECV) and function (as demonstrated by decreased myocardial velocities and twist) may indicate adverse (and perhaps subclinical) effects on the heart.

The goal of this study was to apply structure-function cardiac MRI to explore associations between donor and recipient characteristics and global and regional abnormalities in myocardial tissue structure and function.

Materials and Methods

Study Cohort

A total of 58 HTx recipients (mean age, 51.1 years ± 12.6 [standard deviation]; 26 female patients: 48.9 years ± 14.4, 32 male patients: 53.0 years ± 11.1) were recruited for cardiac MRI from August 2014 to June 2017 at a single tertiary care medical center. Inclusion criteria included the availability of donor characteristics (n = 25 excluded because they were transplanted at other centers). Exclusion criteria included age less than 18 years (n = 0), language barrier (n = 5), decreased capacity to consent (n = 3), or contraindications to cardiac MRI (implanted metallic device, nonretracted lead, claustrophobia, and pregnancy; n = 39). Figure 1 demonstrates the eligibility for inclusion in the study cohort. Cardiac MRI scans were scheduled at variable times throughout transplant follow-up, depending on the availability of the patient. The study cohort overlaps (44 of 58 patients) with a previously published study that examined the differences in cardiac MRI measures between heart transplant recipients and healthy controls and the relationship between structural and functional cardiac MRI measures (20). The study cohort also overlaps (35 of 58 patients) with a previously published study that focused on the detection of ACAR by using cardiac MRI (21). The local institutional review board approved the study, and it was Health Insurance Portability and Accountability Act compliant. Informed consent was obtained from all patients for general analysis of obtained data and available clinical history.

Donor and Recipient Characteristics

The medical records of all study participants were reviewed for relevant donor and recipient characteristics. Donor characteristics included age, sex, height, weight, and body mass index (BMI), as well as potential confounding comorbidities (HTN, DM, and history of smoking). Recipient demographic characteristics included age at transplant, age at scan, sex, height at transplant, weight at transplant, and BMI at transplant. Potential recipient confounding variables included HTN, DM, and history of smoking, as well as history of ACAR (either acute cellular rejection, defined as endomyocardial biopsy grade ≥ 2R, or antibody-mediated rejection, defined as ≥ p-AMR-2 according to the latest International Society of Heart and Lung Transplantation grading scale [22,23]) and CAV (diagnosis based on angiographic/intravascular US findings in medical records). In addition, time since transplant was calculated for analysis as a potential confounding variable for donor and recipient factors. Cold ischemia time during transplantation was also obtained. Given that donor and recipient characteristics were present before recruitment, this study is best characterized as a retrospective observational study.

Cardiac MRI

Cardiac MRI was performed on a 1.5-T MR system (Magnetom Aera or Avanto; Siemens, Erlangen, Germany). All patients underwent cardiac MRI, including electrocardiographically gated two-dimensional SSFP imaging, T2 mapping, precontrast and postcontrast T1 mapping, and TPM. T2 mapping, T1 mapping, and TPM were acquired during breath holding at identical short-axis locations at the base, mid, and apex of the LV (Fig 2).

As shown in Figure 2, *A*, changes in myocardial tissue were assessed by T2 and T1 mapping. T2 mapping was based on the successive acquisition of three T2-prepared SSFP images with varying T2 preparation times (0, 24, and 55 msec) (14). Further imaging parameters were as follows: echo time/repetition time = 1.1–1.4 msec/2.2–2.6 msec, spatial resolution = 1.5–2.1 mm × 2.0–2.5 mm, section thickness = 8 mm, diastolic acquisition window = 270 msec, flip angle = 70°.

T1 mapping consisted of single-shot modified Look-Locker inversion recovery images before and 15 minutes following administration of gadolinium-based contrast material (Magnevist or Gadavist; Bayer, Leverkusen, Germany; 0.1 mmol/kg) (15). Imaging reconstruction included motion correction of the modified Look-Locker inversion recovery images with different inversion times and the calculation of parametric LV T1 maps as described in previous studies (16,17). Patients with glomerular filtration rate (GFR) less than 30 or a recent decline in GFR did not receive gadolinium-based contrast material or contrast material–dependent imaging sequences. Imaging parameters were

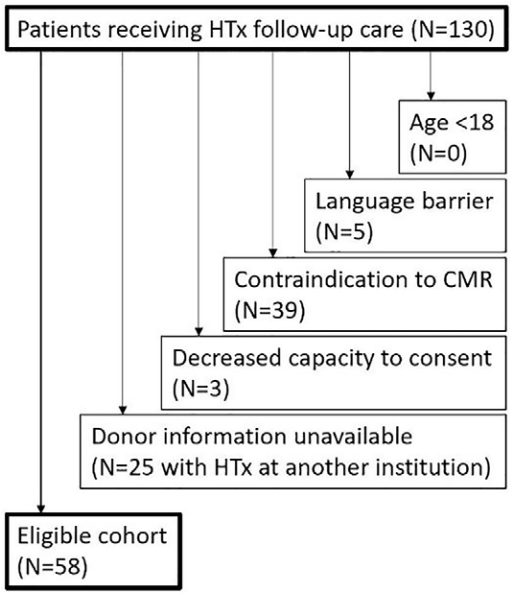

Figure 1: Flowchart shows the eligibility for the study cohort and number of patients meeting exclusion criteria. CMR = cardiac MRI, HTx = heart transplantation.

as follows: echo time/repetition time = 1.0–1.3 msec/2.5–4.2 msec, spatial resolution = 1.0–2.1 mm × 1.5–2.5 mm, section thickness = 8 mm, flip angle = 35°.

As shown in Figure 2, *B*, LV velocities and global function were assessed by using breath-held TPM and two-dimensional cine SSFP imaging. TPM data were acquired in three short-axis locations (base, mid, and apex) to measure myocardial velocities with tridirectional velocity encoding (maximum encoded velocity (venc) = 25 cm/sec) (18,19). Imaging parameters were as follows: temporal resolution = 20.8 msec, spatial resolution = 2.9 × 2.4 mm^2, section thickness = 8 mm, k-t parallel MRI with extended and average generalized autocalibrating partially parallel acquisition kernels (or PEAK GRAPPA) with an acceleration factor of 3.6, and acquisition time per two-dimensional section = 25 heart beats. Cine SSFP MRI data were acquired with the following imaging parameters: echo time/repetition time = 2.8/1.1 msec; flip angle = 65°, in-plane resolution = 2.1 × 2.1 mm^2, bandwidth = 930 Hz per pixel, section thickness = 8 mm, section gap = 50%, to cover the entire LV in 8–10 sections in short-axis location from the apex to base.

Cardiac MRI Data Analysis

Global LV function parameters, including end-diastolic myocardial mass, stroke volume, cardiac output, and ejection fraction, were calculated from cine SSFP images by using commercial software (cvi42, version 5.3.6; Circle, Calgary, Canada).

For analysis of T2, T1, and ECV, the LV was divided into 16 segments by using the American Heart Association 16-segment model (24). Segmental T2 and T1 values were calculated from scanner-generated T2 and precontrast and postcontrast T1 maps by using commercial software (cvi42, version 5.3.6). ECV was calculated during postprocessing on commercial software (cvi42, version 5.3.6) using precontrast and postcontrast T1 maps and the patient hematocrit level obtained on the day of the cardiac MRI scan to determine the segmental ECV using the following equation: ECV = (ΔR1 myocardium/ΔR1 blood) × (1 – hematocrit), where R1 = 1/T1 and ΔR1 is the relaxation rate difference between precontrast and postcontrast T1 images (16). Global T2, T1, and ECV values were calculated as an average of all 16 segmental values (to quantify diffuse elevation of these parameters), and peak values were calculated as the maximal individual segmental value (to quantify more focal increases in these parameters).

TPM data were analyzed by using in-house tools programmed in Matlab (MathWorks, Natick, Mass). Analysis included manual delineation of endocardial and epicardial LV contours and transformation of the acquired tridirectional velocities into radial velocities (representing contraction and expansion), long-axis velocities (LV lengthening and shortening), and circumferential velocities (LV rotation), as described in previous studies (19,25). Peak myocardial velocities during systole and diastole were determined for radial and long-axis directions. LV twist was calculated from the difference between basal and apical circumferential myocardial velocities, allowing for the determination of peak systolic twist and peak diastolic untwist.

Postprocessing analyses were performed by authors (R.S.D. and R.S. with 1 and 4 years of cardiac imaging experience, respectively). The authors were blinded to all characteristic data.

Statistical Analysis

For paired continuous demographic donor-recipient characteristics (age, height, weight, and BMI), relative differences were calculated and normalized to the recipient characteristics. Pearson correlation analyses were performed between continuous characteristic variables (age, height, weight, BMI, and cold ischemia time during transplantation) and cardiac MRI measures (LV mass, stroke volume, cardiac output, ejection fraction, T2, T1, ECV, myocardial velocities, and twist). Multiple linear regression analyses were performed to adjust for confounding variables (HTN, DM, smoking, ACAR, CAV, age, and time since transplant); all confounding variables were tested together, then confounding variables were tested individually if the regression coefficient changed by more than 10%. To test for difference between groups with different categorical characteristic variables (sex, HTN, DM, and smoking history), a Lilliefors test was used to determine parameter normality. For each cardiac MRI measure, appropriate tests (*t* tests for Gaussian distributions and Mann-Whitney tests otherwise) were used for paired comparisons of data between patient groups. A Fisher exact test was used to test for differences between categorical variables. A *P* value less than .05 was considered statistically significant. The analysis was performed by using SPSS (version 23; IBM, Armonk, NY).

Results

Donor and Recipient Characteristics

Donor and recipient characteristics for all HTx recipients are summarized in Tables 1 and 2. HTx recipients were

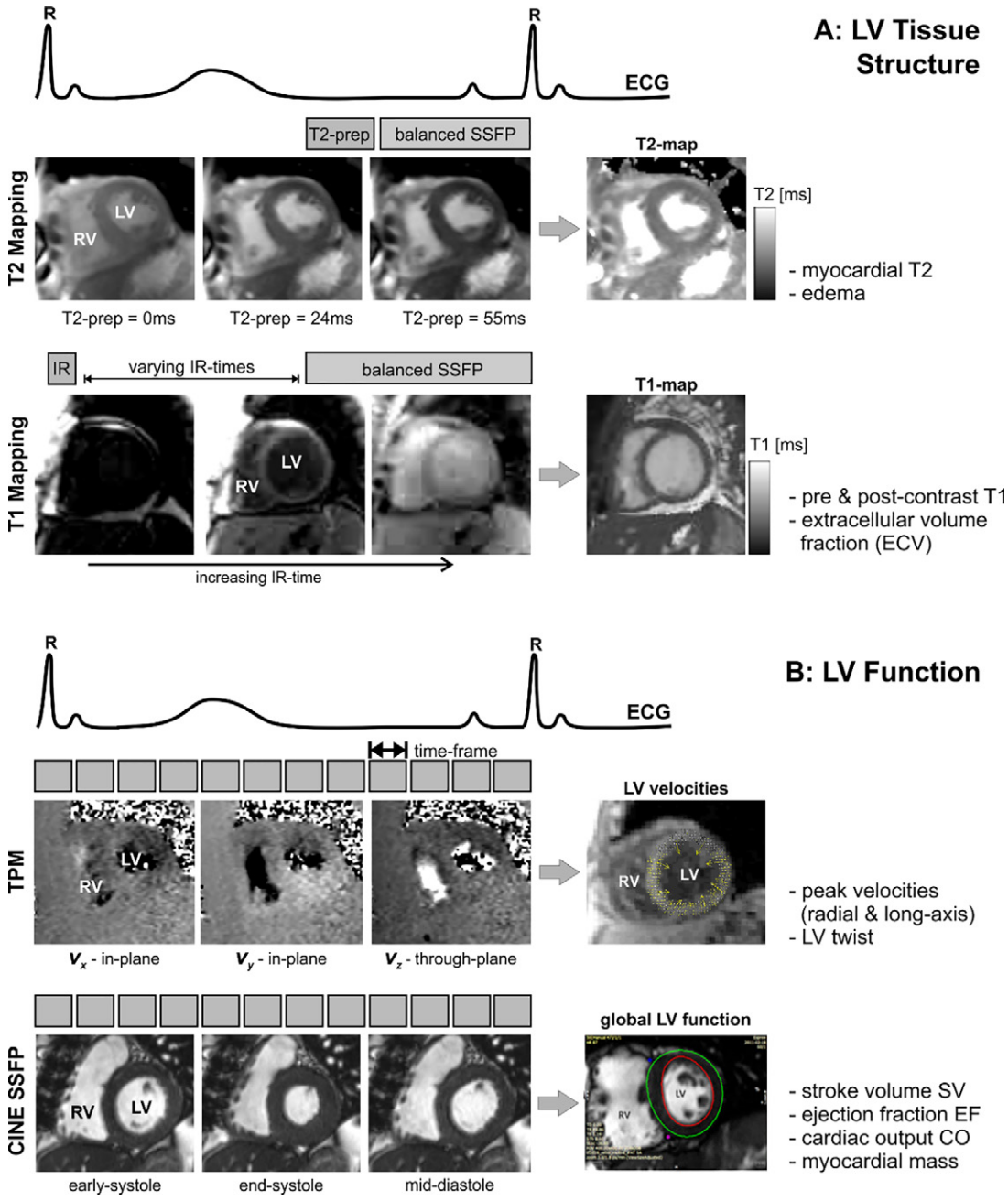

Figure 2: Combined T2 mapping, T1 mapping, tissue phase mapping (TPM), and cine steady-state free precession (SSFP) MRI for the comprehensive evaluation of myocardial, *A*, tissue structure and, *B*, function. T2 mapping is based on diastolic balanced SSFP imaging with different T2 preparation times. T1 mapping uses balanced SSFP imaging with different inversion recovery (IR) times. TPM is based on electrocardiographically (ECG) gated black-blood prepared phase contrast MRI with three-directional velocity encoding. T2 mapping, T1 mapping, and TPM were acquired in short-axis orientation (base, mid, and apex) during breath holding. CO = cardiac output, EF = ejection fraction, LV = left ventricular, prep = preparation time, RV = right ventricular, SV = stroke volume.

significantly older compared with the age of transplanted donor hearts, and HTx recipients were more frequently female (n = 26) compared with the sex of donors (n = 16). A third of recipients (31%) received a heart from a member of the opposite sex. Height, weight, and BMI were similar for HTx recipients and donors; however, a donor-recipient weight mismatch > 20% was found in 28 cases (17 donor weight > recipient weight and 11 recipient weight > donor weight). A total of 16 HTx patients (28%) demonstrated a history of ACAR (none with active ACAR at the time of cardiac MRI per endomyocardial biopsy, average 2.54 years later) and 10 (17%) had a history of CAV. Cardiac MRI was performed 3.9 years ± 2.9 (range, 1 month to 10 years) following transplant. In total, 11 patients did not receive gadolinium-based contrast material due to GFR < 30 or a recent decline in GFR; postcontrast T1 mapping data and ECV were thus available in 47 patients. TPM was performed in a subgroup of 45 HTx recipients.

Table 1: Heart Transplantation Recipient and Donor Characteristics of 58 Patients

Characteristic	Recipient (n = 58)	Donor (n = 58)	Recipient-Donor Difference*	P Value
Age at HTx (y)	51.1 ± 12.6	27.8 ± 11.0	24.2 ± 13.5 (46%)	<.001
Age at cardiac MRI (y)	55.8 ± 15.2	NA	NA	NA
Male:female ratio	32:26	42:16	18 (31%) discordant	.082
Height (cm)	173.5 ± 10.8	174.2 ± 8.7	7.8 ± 6.1 (5%)	.597
Weight (kg)	79.2 ± 15.8	75.8 ± 15.0	18.8 ± 14.8 (19%)	.155
BMI (kg/m^2)	26.2 ± 4.3	25.3 ± 5.0	4.7 ± 3.0 (19%)	.276
Hypertension	50 (86)	8 (14)	NA	NA
Diabetes	31 (53)	2 (3)	NA	NA
Smoking history	30 (52)	3 (5)	NA	NA
Cold ischemia time during transplantation (h)	2.8 ± 1.2	NA	NA	NA
History of ACAR	16 (28)	NA	NA	NA
History of CAV	10 (17)	NA	NA	NA

Note.—Values are means ± standard deviation or number of patients with percentages in parentheses, unless otherwise indicated. Percentage differences in age, height, weight, and BMI are normalized to recipient. ACAR = acute cardiac allograft rejection, BMI = body mass index, CAV = cardiac allograft vasculopathy, HTx = heart transplantation, NA = not applicable.
* For age at HTx, height, weight, and BMI, the percentage in parentheses is percentage difference between recipient and donor. For male:female ratio, the percentage is the percentage of donor-recipient matches with discordant sexes (female donor with male recipient or male donor with female recipient).

Impact of Donor and Recipient Sex on LV Tissue and Function

As summarized in Table 3, stroke volume, cardiac output, and LV mass were increased ($P < .02$) for male HTx recipients compared with female HTx recipients. Myocardial tissue parameters demonstrated increased global precontrast T1 ($P = .002$) and peak T1 ($P = .014$) for female HTx recipients. In addition, systolic peak long-axis velocities were reduced for female subjects ($P = .015$). In contrast, donor sex was less impactful and only resulted in differences in LV mass (female donor: 76.8 g ± 22.8; male donor 101.3 g ± 25.3; $P = .001$). Donor-recipient sex mismatch resulted in ejection fraction differences (sex mismatch: 66.1% ± 12.9; sex match: 60.3% ± 10.6; $P = .019$).

Impact of Donor and Recipient Age, Weight, and Height on LV Tissue and Function

Increased HTx recipient age (Fig 3, *A*) was associated with impaired diastolic peak velocities along both radial and long-axis LV motion directions ($r = 0.40$ and $r = 0.27$, respectively; $P < .05$). In addition, there were significant relationships between increased HTx recipient height, weight, and BMI with increased myocardial mass ($r = 0.32$–0.45; $P < .05$). Furthermore, HTx recipient height was positively associated with cardiac output ($r = 0.44$; $P < .01$) and stroke volume ($r = 0.45$; $P < .01$). Multivariate analysis confirmed that none of these relationships were confounded by recipient HTN, DM, smoking history, ACAR, or CAV.

As shown in Figure 3, *B*, increased age of the donor heart resulted in elevated T2, possibly indicating increased edema or inflammation ($r = 0.32$; $P < .05$), and higher ECV, indicating increased interstitial expansion potentially caused by LV fibrosis ($r = 0.47$; $P < .01$). Multivariate analysis showed that the relationship between increased donor age and higher ECV was confounded by the presence of donor HTN ($\beta = .153$, $P < .01$ using simple linear regression; donor age $\beta = .106$, $P = .03$ and donor HTN $\beta = 3.422$, $P = .03$ using multiple linear regression). DM, smoking, ACAR, and CAV were not confounding factors; elevated T2 was not confounded by any donor factor. In addition, increased donor age correlated with reduced diastolic peak long-axis LV velocities ($r = 0.41$; $P < .01$) and reduced diastolic peak untwisting motions of the heart ($r = 0.40$; $P < .01$), which were not confounded by donor factors. Finally, donor BMI demonstrated a positive relationship with increased global and peak ECV ($r = 0.34$–0.36; $P < .01$), which was confounded by donor HTN ($\beta = .344$; $P = .01$ using simple linear regression; donor BMI $\beta = .269$, $P = .03$ and donor HTN $\beta = 4.371$, $P < .01$ using multiple linear regression).

Donor-recipient mismatches in age, weight, and BMI were significantly associated with changes in myocardial ECV (Fig 3, *C*). Notably, elevated ECV was found for older donors (donor age > HTx recipient age) while younger donors (donor age < HTx recipient age, majority of patients) had lower ECV ($r = 0.48$; $P < .01$). Similar correlations with increased ECV were found for donor-recipient weight difference ($r = 0.45$; $P < .01$) and BMI difference ($r = 0.36$; $P < .01$). Each of these relationships with ECV was confounded by donor HTN (weight difference: $\beta = .061$, $P < .01$ using simple linear regression; weight difference $\beta = .042$, $P = .05$ and donor HTN $\beta = 4.095$, $P < .01$ using multiple linear regression; BMI difference: $\beta = .062$, $P = .01$ using simple linear regression; BMI difference $\beta = .054$, $P = .02$ and donor HTN $\beta = 4.521$, $P < .01$ using multiple linear regression).

Impact of Cardiovascular Comorbidities on LV Tissue and Function

As shown in Figure 4, HTN in donors resulted in elevated global ECV (31.0% ± 4.2 vs 26.0% ± 3.3, $P = .001$) and peak ECV (36.1% ± 6.0 vs 30.1% ± 4.0, $P = .001$).

Impact of Recipient History of ACAR and CAV on LV Tissue and Function

HTx recipients with a proven history of ACAR demonstrated elevated myocardial T2 compared with patients without prior

Table 2: Comparisons of Characteristics between Female and Male Heart Transplantation Recipients

Parameter	Female HTx Recipient (*n* = 26)	Male HTx Recipient (*n* = 32)	*P* Value
Sex mismatch	14 (54)	4 (13)	<.001
Age at HTx (y)	48.9 ± 14.4	53.0 ± 11.1	.229
Donor age (y)	26.3 ± 10.6	28.9 ± 11.3	.368
Diff age (%)	43.5 ± 24.8	43.0 ± 24.2	.932
Height (cm)	165.7 ± 8.2	179.9 ± 8.2	<.001
Donor height (cm)	170.5 ± 8.8	177.2 ± 7.5	.002
Diff height (%)	3.1 ± 7.4	1.4 ± 3.3	.003
Weight (kg)	69.6 ± 12.6	87.1 ± 13.6	<.001
Donor weight (kg)	71.4 ± 13.7	79.3 ± 15.4	.046
Diff weight (%)	5.1 ± 25.0	7.3 ± 21.9	.049
BMI (kg/m^2)	24.9 ± 4.0	27.2 ± 4.4	.047
Donor BMI (kg/m^2)	24.6 ± 4.6	25.8 ± 5.2	.375
Diff BMI (%)	1.9 ± 22.7	3.6 ± 21.2	.353
Hypertension	21 (81)	29 (91)	.283
Donor hypertension	3 (12)	6 (19)	.455
Diabetes	7 (27)	14 (44)	.189
Donor diabetes	1 (4)	1 (3)	.882
Smoking history	11 (42)	19 (59)	.200
Donor smoking history	1 (4)	2 (6)	.684
Cold ischemia time during transplantation (h)	3.0 ± 0.7	3.2 ± 0.7	.373
History of ACAR	7 (27)	8 (25)	.869
History of CAV	3 (12)	7 (22)	.304

Note.—Values are means ± standard deviations or number of patients with percentages in parentheses, unless otherwise indicated. Percent differences in age, height, weight, and BMI are normalized to recipient (|(donor characteristic–recipient characteristic)|/recipient characteristic). ACAR = acute cardiac allograft rejection, BMI = body mass index, CAV = cardiac allograft vasculopathy, Diff = difference, HTx = heart transplantation.

Table 3: Differences in Cardiac Tissue Structure and Myocardial Function Parameters of Heart Transplant Recipients Based on Sex

HTx recipient	Female Recipient (*N* = 26)	Male Recipient (*N* = 32)	*P* Value
Global LV function			
Heart rate (bpm)	90.0 ± 14.5	90.3 ± 12.7	.938
Stroke volume (mL)	63.4 ± 19.0	77.7 ± 18.8	.007
Cardiac output (L/min)	5.7 ± 1.7	6.8 ± 1.7	.017
EF (%)	63.1 ± 14.2	61.1 ± 8.9	.116
LV mass (g)	76.8 ± 22.8	101.3 ± 25.3	.001
LV tissue structure			
Global T2 (msec)	51.7 ± 3.9	50.0 ± 5.3	.158
Peak T2 (msec)	57.1 ± 4.8	55.9 ± 6.9	.453
Global T1 (msec)	1067.2 ± 58.3	1024.6 ± 62.3	.002
Peak T1 (msec)	1130.4 ± 68.5	1099.5 ± 99.2	.014
Global ECV (%)*	27.4 ± 4.5	26.3 ± 3.3	.369
Peak ECV (%)*	31.6 ± 5.1	30.5 ± 4.6	.462
LV velocities			
Peak radial velocity—systole (cm/sec)†	2.56 ± 0.40	2.64 ± 0.43	.520
Peak radial velocity—diastole (cm/sec)†	−4.11 ± 1.05	−3.82 ± 0.84	.306
Peak long-axis velocity—systole (cm/sec)†	2.53 ± 0.88	3.25 ± 1.00	.015
Peak long-axis velocity—diastole (cm/sec)†	−3.25 ± 1.03	−3.10 ± 1.09	.632
LV peak twist—systole (cm/sec)†	2.17 ± 0.55	2.20 ± 0.80	.917
LV peak untwist—diastole (cm/sec)†	−2.93 ± 0.94	−2.90 ± 0.83	.921

Note.—Values are means ± standard deviations. ECV = extracellular volume fraction, EF = ejection fraction, HTx = heart transplantation, LV = left ventricular.
* ECV calculation was performed in 20 female and 27 male HTx recipients.
† Peak velocity and twist calculations were performed in 23 female and 22 male HTx recipients.

ACAR (53.3 msec ± 4.8 vs 49.8 msec ± 4.4, *P* = .001). The presence of CAV did not result in any significant differences in LV tissue or function parameters.

Discussion

Our study demonstrated that donor and recipient characteristics are associated with differences in cardiac MRI–derived measures of global and regional myocardial structure and function. To our knowledge, this is the first dedicated study to examine the relationships between cardiac MRI measures of cardiac health and donor and recipient characteristics following HTx, including sex, age, height, weight, BMI, and HTN.

Sex had a strong impact on cardiac MRI measures of myocardial tissue and function. Male recipients demonstrated higher myocardial mass than female recipients, which is consistent with prior studies in the general population (11,12). Female transplant recipients displayed significantly higher T1, similar to findings from prior studies in the general population (26,27). In addition, female recipients demonstrated reduced systolic long-axis myocardial peak velocities compared with male recipients. Lower systolic long-axis velocities in female recipients may in part be explained by having smaller hearts, but decreased myocardial mass and increased T1 may be related to different hormonal and myocyte responses to cardiovascular stress (28).

Several global and regional structural and functional parameters were associated with the ages of the recipient and donor.

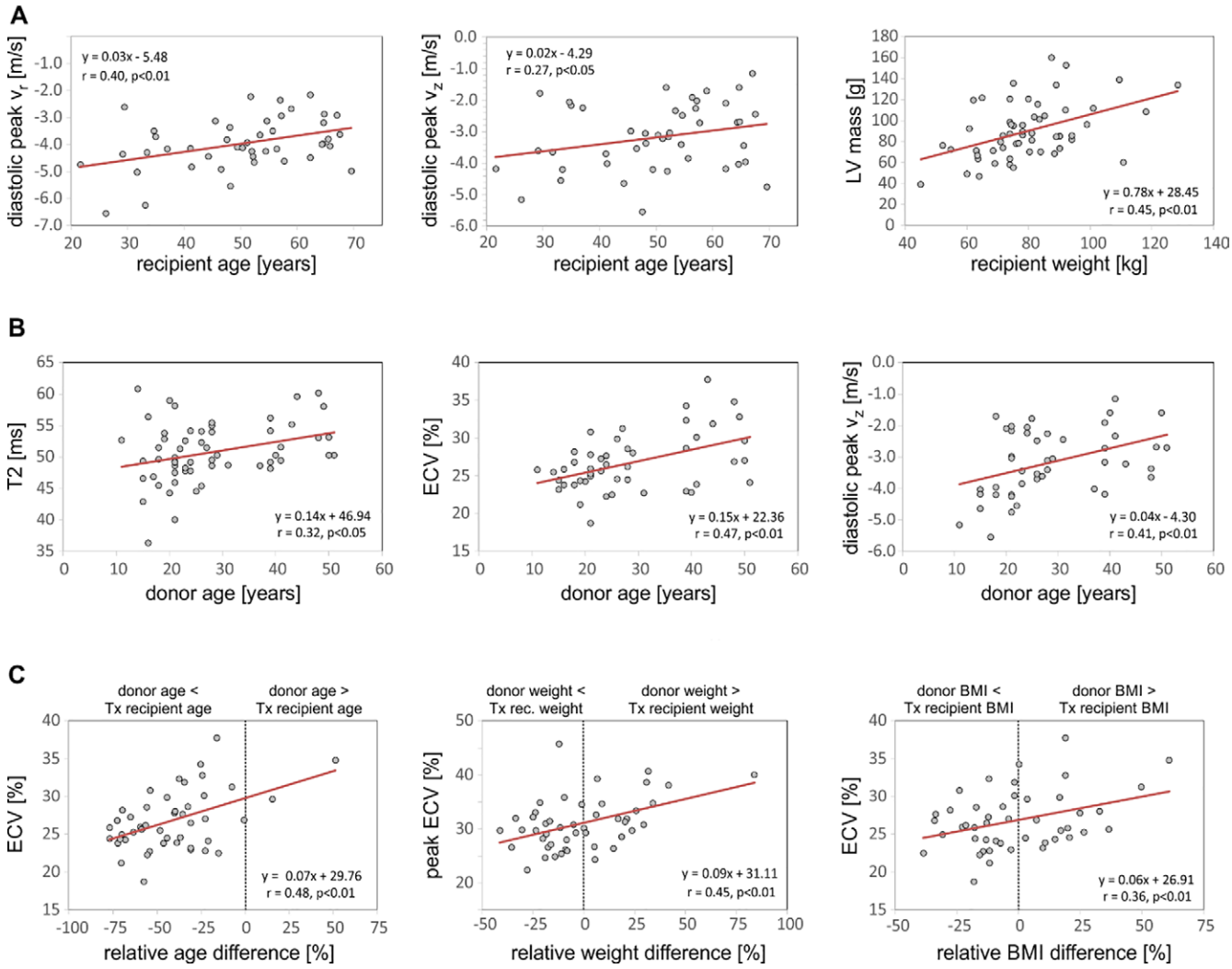

Figure 3: Correlation analysis of the impact of, *A*, heart transplant recipient characteristics, *B*, donor characteristics, and, *C*, donor-recipient differences on myocardial tissue structure and function. BMI = body mass index, ECV = extracellular volume fraction, LV = left ventricular, Tx = treatment, V_r = radial velocity, V_z = longitudinal velocity.

Higher donor age was associated with higher T2 and ECV, suggestive of increased interstitial edematous and/or fibrotic change in older donor hearts, possibly related to increasing cardiovascular comorbidities with age (such as HTN; donor age was not associated with ACAR). Prior studies in the general population have also demonstrated positive correlations between age and T2 (26) and ECV (27,29), but no studies have specifically examined the impact of donor age in the transplant population. Donor age also correlated with the decreasing magnitude of diastolic long-axis velocities and diastolic LV twist, suggestive of diastolic dysfunction. Diastolic dysfunction is a common complication following HTx and is associated with increased mortality (30). In addition, our findings support prior studies that found correlations between increased heart age and reduced diastolic myocardial velocities in the general population and in transplant recipients (18).

Recipient and donor body size demonstrated significant relationships with global structural and functional parameters. Recipient height, weight, and BMI were positively associated with myocardial mass, as has been shown in echocardiography in the general population (31). These associations between demographic characteristics and global myocardial structural parameters are logical physiologically; larger patients demonstrated higher myocardial mass. Interestingly, LV mass correlated with recipient body size and not donor body size, suggestive of myocardial remodeling to adapt to the physiology of the heart recipient following transplant. Global functional parameters also demonstrated expected results. Recipient height was positively associated with cardiac output and stroke volume. Correlations between height and cardiac output and stroke volume have been shown in prior echocardiography studies (32); taller patients have greater intravascular volume and require greater cardiac output, accomplished with higher stroke volumes instead of heart rate.

Recipient and donor body size was also associated with several regional structural and functional parameters. Donor BMI was positively associated with ECV, which was found to be confounded by donor HTN. In a prior study of obese diabetic and nondiabetic adolescents, BMI was also associated with ECV, even after adjusting for HTN (33). These subtle alterations to

the myocardial interstitium preceded LV dysfunction, as has been shown in the pediatric heart transplant population (34). Our findings are consistent with prior studies in other populations, demonstrating changes to the extracellular matrix with obesity.

Increased differences in donor versus recipient BMI, weight, and age were significantly correlated with increased ECV, which were influenced by donor HTN. These relationships indicate that a donor-recipient mismatch was associated with signs of myocardial interstitial expansion, possibly representing fibrosis. Changes in ECV may contribute toward worse outcomes associated with size-mismatched and age-mismatched hearts (7).

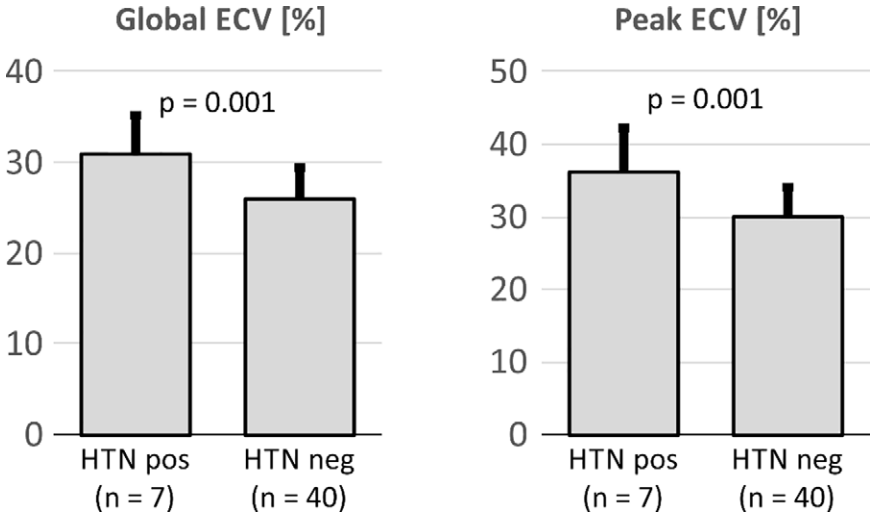

Figure 4: Global and peak extracellular volume fraction (ECV) for transplanted hearts obtained from donors with history of hypertension (HTN pos) compared with donors without hypertension (HTN neg).

History of ACAR in HTx recipients also resulted in elevated myocardial T2, which is in line with previous studies. T2 mapping has shown the most consistent correlation with ACAR, with sensitivity and specificity as high as 72%–89% and 91%–96%, respectively (13,35).

Overall, our study demonstrated that myocardial tissue structure and function are influenced by numerous donor and recipient factors, including age, sex, height, weight, BMI, and HTN. Most transplant centers restrict donor age (commonly to less than 55 years) and use body weight to match cardiac sizes (2,7). Some centers prefer male donors, given that the majority of transplant recipients are men and studies demonstrate worse outcomes in male recipients of female hearts (4,6). While current practice accounts for age and weight and often considers sex, additional factors such as height and BMI are not included in sizing considerations, which may lead to substantial sizing discrepancies. Our findings of significant differences in cardiac output, myocardial edema (T2), interstitial expansion (ECV), and impaired regional diastolic function based on height, weight, and BMI support recent work in advancing models combining all of these factors for improved size matching (2,5,7).

Even though our study finds several associations between donor and recipient characteristics and cardiac MRI parameters, it is important to note several limitations. First, although we included important donor and recipient cardiovascular comorbidities to test for confounding variables with age, weight, and BMI, there may be additional confounding factors that were not included. Potential confounding comorbidities did not result in differences in myocardial tissue and function, except for donor HTN, which resulted in elevated ECV in the transplanted hearts. However, this finding is based on a small cohort of donors with HTN (n = 8) in our cohort, and further study of this finding in a larger group of HTx patients is suggested. In addition, other risk factors and comorbidities considered in determining a donor's suitability, such as drug use, HIV status, and viral hepatitis, could be examined. Second, this study was also limited by using a single cardiac MRI, on average 4 years after HTx. Early cardiac MRI assessment in the first months after HTx and at a second point later may provide additional valuable information of longitudinal changes in cardiac structure and function related to recipient characteristics that could not be assessed with our study design. In this study, we used regression analysis to demonstrate associations over our entire sample; however, future longitudinal studies demonstrating change over time would be best for analyzing cases on an individual basis. Third, data regarding ECV (not performed in patients unable to receive contrast material) and TPM-derived myocardial velocities and twist (TPM sequences not included in earliest cardiac MRI studies) were not available across all patients in the cohort, decreasing our sample size for certain analyses. In addition, the inclusion of other validated structural and functional cardiac MRI sequences, such as late gadolinium enhancement, myocardial perfusion, and deformation techniques (strain) (36), would provide a more comprehensive regional analysis of the heart. Although late gadolinium enhancement is a well-validated measure of focal scar formation, we use calculation of ECV as an alternative measure of diffuse and focal interstitial expansion (and potentially scar formation).

In conclusion, donor and recipient characteristics influence cardiac MRI–derived myocardial structural and functional change following HTx. Further longitudinal studies are warranted to evaluate the role of the findings in our study cohort with regard to adverse outcomes observed with donor and recipient characteristics.

Author contributions: Guarantors of integrity of entire study, R.S.D., M.M.; study concepts/study design or data acquisition or data analysis/interpretation, all authors; manuscript drafting or manuscript revision for important intellectual content, all authors; approval of final version of submitted manuscript, all authors; agrees to ensure any questions related to the work are appropriately resolved, all authors; literature research, R.S.D., A.A.R., R.S., K.G., S.S.K., J.D.R., C.W.Y., J.C.C., M.M.; clinical studies, R.S.D., A.A.R., J.B., R.S., J.E.W., J.D.R., A.S.A., J.C.C., M.M.; statistical analysis, R.S.D., J.B., J.C.C., M.M.; and manuscript editing, R.S.D., A.A.R., J.B., K.G., J.E.W., S.S.K., E.E.V., J.D.R., C.W.Y., A.S.A., J.C.C., M.M.

Disclosures of Conflicts of Interest: R.S.D. disclosed no relevant relationships. **A.A.R.** disclosed no relevant relationships. **J.B.** disclosed no relevant relationships. **R.S.** disclosed no relevant relationships. **K.G.** disclosed no relevant relationships. **J.E.W.** Activities related to the present article: disclosed no relevant relationships.

Activities not related to the present article: has given expert testimony on the use of wideband cardiac MRI to predict right ventricular failure after LVAD; institution has AHA Innovation Award and NIH RO1 award, both pending July 1; is on the speakers bureaus of Boehringer Ingelheim Pharmaceuticals and Medtronic. Other relationships: disclosed no relevant relationships. **S.S.K.** disclosed no relevant relationships. **E.E.V.** disclosed no relevant relationships. **J.D.R.** disclosed no relevant relationships. **C.W.Y.** disclosed no relevant relationships. **A.S.A.** disclosed no relevant relationships. **J.C.C.** Activities related to the present article: disclosed no relevant relationships. Activities not related to the present article: is a consultant for Bayer, Circle, Siemens, and GE; institution has grants or grants pending with Bayer, Guerbet, and Siemens; is on the speakers bureaus of Circle and Guerbet; has received payment of travel/accommodations/meeting expenses from Siemens, GE, Circle, Guerbet, and Bayer. Other relationships: disclosed no relevant relationships. **M.M.** Activities related to the present article: disclosed no relevant relationships. Activities not related to the present article: is a consultant for Circle Cardiovascular Imaging; institution has grants or grants pending with Circle Cardiovascular Imaging, Cryolife, and Siemens Healthineers. Other relationships: disclosed no relevant relationships.

References

1. Katz JN, Waters SB, Hollis IB, Chang PP. Advanced therapies for end-stage heart failure. Curr Cardiol Rev 2015;11(1):63–72.
2. Kilic A, Emani S, Sai-Sudhakar CB, Higgins RS, Whitson BA. Donor selection in heart transplantation. J Thorac Dis 2014;6(8):1097–1104.
3. Smits JM, De Pauw M, de Vries E, et al. Donor scoring system for heart transplantation and the impact on patient survival. J Heart Lung Transplant 2012;31(4):387–397.
4. Khush KK, Kubo JT, Desai M. Influence of donor and recipient sex mismatch on heart transplant outcomes: analysis of the International Society for Heart and Lung Transplantation Registry. J Heart Lung Transplant 2012;31(5):459–466.
5. Patel ND, Weiss ES, Nwakanma LU, et al. Impact of donor-to-recipient weight ratio on survival after heart transplantation: analysis of the United Network for Organ Sharing Database. Circulation 2008;118(14 Suppl):S83–S88.
6. Weiss ES, Allen JG, Patel ND, et al. The impact of donor-recipient sex matching on survival after orthotopic heart transplantation: analysis of 18 000 transplants in the modern era. Circ Heart Fail 2009;2(5):401–408.
7. Reed RM, Netzer G, Hunsicker L, et al. Cardiac size and sex-matching in heart transplantation: size matters in matters of sex and the heart. JACC Heart Fail 2014;2(1):73–83.
8. Weber DJ, Wang IW, Gracon AS, et al. Impact of donor age on survival after heart transplantation: an analysis of the United Network for Organ Sharing (UNOS) registry. J Card Surg 2014;29(5):723–728.
9. Khan AM, Green RS, Lytrivi ID, Sahulee R. Donor predictors of allograft utilization for pediatric heart transplantation. Transpl Int 2016;29(12):1269–1275.
10. Khush KK, Menza R, Nguyen J, Zaroff JG, Goldstein BA. Donor predictors of allograft use and recipient outcomes after heart transplantation. Circ Heart Fail 2013;6(2):300–309.
11. Kawel N, Turkbey EB, Carr JJ, et al. Normal left ventricular myocardial thickness for middle-aged and older subjects with steady-state free precession cardiac magnetic resonance: the multi-ethnic study of atherosclerosis. Circ Cardiovasc Imaging 2012;5(4):500–508.
12. Petersen SE, Aung N, Sanghvi MM, et al. Reference ranges for cardiac structure and function using cardiovascular magnetic resonance (CMR) in Caucasians from the UK Biobank population cohort. J Cardiovasc Magn Reson 2017;19(1):18.
13. Bonnemains L, Villemin T, Escanye JM, et al. Diagnostic and prognostic value of MRI T2 quantification in heart transplant patients. Transpl Int 2014;27(1):69–76.
14. Giri S, Chung YC, Merchant A, et al. T2 quantification for improved detection of myocardial edema. J Cardiovasc Magn Reson 2009;11(1):56.
15. Messroghli DR, Radjenovic A, Kozerke S, Higgins DM, Sivananthan MU, Ridgway JP. Modified Look-Locker inversion recovery (MOLLI) for high-resolution T1 mapping of the heart. Magn Reson Med 2004;52(1):141–146.
16. Kellman P, Wilson JR, Xue H, Ugander M, Arai AE. Extracellular volume fraction mapping in the myocardium, part 1: evaluation of an automated method. J Cardiovasc Magn Reson 2012;14(1):63.
17. Kellman P, Wilson JR, Xue H, et al. Extracellular volume fraction mapping in the myocardium, part 2: initial clinical experience. J Cardiovasc Magn Reson 2012;14(1):64.
18. Föll D, Jung B, Schilli E, et al. Magnetic resonance tissue phase mapping of myocardial motion: new insight in age and gender. Circ Cardiovasc Imaging 2010;3(1):54–64.
19. Jung B, Föll D, Böttler P, Petersen S, Hennig J, Markl M. Detailed analysis of myocardial motion in volunteers and patients using high-temporal-resolution MR tissue phase mapping. J Magn Reson Imaging 2006;24(5):1033–1039.
20. Dolan RS, Rahsepar AA, Blaisdell J, et al. Cardiac structure-function MRI in patients after heart transplantation. J Magn Reson Imaging 2019;49(3):678–687.
21. Dolan RS, Rahsepar AA, Blaisdell J, et al. Multiparametric cardiac magnetic resonance imaging can detect acute cardiac allograft rejection after heart transplantation. JACC Cardiovasc Imaging 2019;12(8 Pt 2):1632–1641.
22. Costanzo MR, Dipchand A, Starling R, et al. The International Society of Heart and Lung Transplantation Guidelines for the care of heart transplant recipients. J Heart Lung Transplant 2010;29(8):914–956.
23. Berry GJ, Burke MM, Andersen C, et al. The 2013 International Society for Heart and Lung Transplantation Working Formulation for the standardization of nomenclature in the pathologic diagnosis of antibody-mediated rejection in heart transplantation. J Heart Lung Transplant 2013;32(12):1147–1162.
24. Cerqueira MD, Weissman NJ, Dilsizian V, et al. Standardized myocardial segmentation and nomenclature for tomographic imaging of the heart. A statement for healthcare professionals from the Cardiac Imaging Committee of the Council on Clinical Cardiology of the American Heart Association. Circulation 2002;105(4):539–542.
25. Markl M, Schneider B, Hennig J. Fast phase contrast cardiac magnetic resonance imaging: improved assessment and analysis of left ventricular wall motion. J Magn Reson Imaging 2002;15(6):642–653.
26. Bönner F, Janzarik N, Jacoby C, et al. Myocardial T2 mapping reveals age- and sex-related differences in volunteers. J Cardiovasc Magn Reson 2015;17(1):9.
27. Liu CY, Liu YC, Wu C, et al. Evaluation of age-related interstitial myocardial fibrosis with cardiac magnetic resonance contrast-enhanced T1 mapping: MESA (Multi-Ethnic Study of Atherosclerosis). J Am Coll Cardiol 2013;62(14):1280–1287.
28. Olivetti G, Giordano G, Corradi D, et al. Gender differences and aging: effects on the human heart. J Am Coll Cardiol 1995;26(4):1068–1079.
29. Ugander M, Oki AJ, Hsu LY, et al. Extracellular volume imaging by magnetic resonance imaging provides insights into overt and sub-clinical myocardial pathology. Eur Heart J 2012;33(10):1268–1278.
30. Tallaj JA, Kirklin JK, Brown RN, et al. Post-heart transplant diastolic dysfunction is a risk factor for mortality. J Am Coll Cardiol 2007;50(11):1064–1069.
31. Foppa M, Duncan BB, Rohde LE. Echocardiography-based left ventricular mass estimation. How should we define hypertrophy? Cardiovasc Ultrasound 2005;3(1):17.
32. Collis T, Devereux RB, Roman MJ, et al. Relations of stroke volume and cardiac output to body composition: the strong heart study. Circulation 2001;103(6):820–825.
33. Shah RV, Abbasi SA, Neilan TG, et al. Myocardial tissue remodeling in adolescent obesity. J Am Heart Assoc 2013;2(4):e000279.
34. Feingold B, Salgado CM, Reyes-Múgica M, et al. Diffuse myocardial fibrosis among healthy pediatric heart transplant recipients: correlation of histology, cardiovascular magnetic resonance, and clinical phenotype. Pediatr Transplant 2017;21(5):e12986.
35. Usman AA, Taimen K, Wasielewski M, et al. Cardiac magnetic resonance T2 mapping in the monitoring and follow-up of acute cardiac transplant rejection: a pilot study. Circ Cardiovasc Imaging 2012;5(6):782–790.
36. Erbel C, Mukhammadaminova N, Gleissner CA, et al. Myocardial perfusion reserve and strain-encoded CMR for evaluation of cardiac allograft microvasculopathy. JACC Cardiovasc Imaging 2016;9(3):255–266.